

# Preparation and Properties of Magnesium, Calcium, Strontium, and Barium Selenolates and Tellurolates

David E. Gindelberger and John Arnold\*

Department of Chemistry, University of California, Berkeley, California 94720

Received July 14, 1994<sup>®</sup>

The sterically encumbered silyl ligands  $-\text{ESi}(\text{SiMe}_3)_3$  ( $\text{E} = \text{Se}, \text{Te}$ ) have been used to prepare the first well-characterized examples of group 2 selenolates and tellurolates. Reaction of  $\text{HSeSi}(\text{SiMe}_3)_3$  with either dibutylmagnesium or the bis(trimethylsilyl)amides of calcium, strontium and barium in the presence of Lewis bases yielded crystalline alkaline earth selenolates. The magnesium selenolate was crystallized as a TRMPSI complex (TRMPSI = tris((dimethylphosphino)methyl)-*tert*-butylsilane), while the calcium, strontium and barium compounds were isolated as TMEDA adducts (TMEDA = *N,N,N',N'* tetramethylethylenediamine). Tellurololysis of dibutylmagnesium in hexane gave the base-free, homoleptic tellurolate compound  $\text{Mg}[\text{TeSi}(\text{SiMe}_3)_3]_2$  as colorless plates in high yield. The bis-THF derivative, prepared by recrystallization in the presence of THF, has been characterized by X-ray crystallography. Reactions between the same group 2 silylamides and two equivalents of  $\text{HTeSi}(\text{SiMe}_3)_3$  in hexane gave high yields of the corresponding tellurolate complexes of calcium, strontium, and barium, that were isolated and crystallized as their THF adducts. The analogous pyridine complexes were readily prepared by the same reactions in the presence of pyridine. Treatment of the bis(pyridine)magnesium tellurolate with 12-crown-4 results in displacement of both the pyridine and the tellurolate ligands to form the ionic complex  $[\text{Mg}(12\text{-C-}4)_2][\text{TeSi}(\text{SiMe}_3)_3]_2$ . X-ray data are as follows:  $[\text{Mg}[\text{SeSi}(\text{SiMe}_3)_3]_2(\text{TRMPSI})]$ , space group  $P2_1/n$ ,  $a = 13.905(7)$  Å,  $b = 15.975(5)$  Å,  $c = 22.55(1)$  Å,  $\beta = 91.77(3)^\circ$ ,  $V = 5674(6)$  Å<sup>3</sup>,  $Z = 4$ ;  $[\text{Sr}[\text{SeSi}(\text{SiMe}_3)_3]_2(\text{TMEDA})_2]$ , space group  $P2_1/c$ ,  $a = 9.388(3)$  Å,  $b = 12.322(4)$  Å,  $c = 23.65(1)$  Å,  $\beta = 95.91(3)^\circ$ ,  $V = 2724(3)$  Å<sup>3</sup>,  $Z = 4$ ;  $[\text{Ba}[\text{TeSi}(\text{SiMe}_3)_3]_2(\text{pyridine})_5]$ , space group  $C2/c$ ,  $a = 13.630(2)$  Å,  $b = 15.933(2)$  Å,  $c = 30.363(4)$  Å,  $\beta = 97.41(1)^\circ$ ,  $V = 6538(2)$  Å<sup>3</sup>,  $Z = 4$ .

## Introduction

Research into the chemistry of group 2 complexes with covalent bonds to group 16 elements has focused almost exclusively on alkoxide and  $\beta$ -diketonate derivatives,<sup>1</sup> while little attention has been given to analogous complexes involving the heavier chalcogens. Although it has been known for some time that tellurium inserts into reactive Mg–carbon bonds to form species that function as useful synthons in organotellurium chemistry,<sup>2–6</sup> to-date there are no reports of well-defined

magnesium tellurolates or selenolates and, consequently, nothing is known regarding their structures and properties.

Recently we reported the preparation of some remarkably stable alkali metal tellurolate derivatives based on sterically hindered  $-\text{ESi}(\text{SiMe}_3)_3$  ligands ( $\text{E} = \text{Se}, \text{Te}$ ) along with studies demonstrating their significant synthetic potential.<sup>7,8</sup> Extending this chemistry to group 2, we have now been able to prepare the first isolable, well-characterized examples of selenolate and tellurolate derivatives of Mg, Ca, Sr, and Ba. In a preliminary account of some of this chemistry, we reported brief synthetic details and the X-ray structures of  $\text{Mg}[\text{TeSi}(\text{SiMe}_3)_3]_2(\text{THF})_2$  and  $\text{Ca}[\text{TeSi}(\text{SiMe}_3)_3]_2(\text{THF})_4$ .<sup>9</sup> Becker and co-workers have subsequently reported an identical preparation and structural characterization of the calcium complex.<sup>10</sup> Tellurolate and selenolate derivatives of strontium or barium are, to the best of our knowledge, unknown.

## Results and Discussion

**Mg Derivatives.** Earlier reports described chalcogen insertions into reactive Mg–C bonds;<sup>2–6</sup> a related approach could not be taken in our case as the required bis(silyl)magnesium starting materials are unknown. Metathesis reactions between

<sup>®</sup> Abstract published in *Advance ACS Abstracts*, November 1, 1994.

- (1) (a) For alkoxides, see for example: Caulton, K. G.; Chisholm, M. H.; Drake, S. R.; Folting, K.; Huffman, J. C.; Streib, W. E. *Inorg. Chem.* **1993**, *32*, 1970. Drake, S. R.; Streib, W. E.; Folting, K.; Chisholm, M. H.; Caulton, K. G. *Inorg. Chem.* **1992**, *31*, 3205. Coan, P. S.; Streib, W. E.; Caulton, K. G. *Inorg. Chem.* **1991**, *30*, 5019. Drake, S. R.; Streib, W. E.; Chisholm, M. H.; Caulton, K. G. *Inorg. Chem.* **1990**, *29*, 2707. Caulton, K. G.; Chisholm, M. H.; Drake, S. R.; Huffman, J. C. *J. Chem. Soc., Chem. Comm.* **1990**, 1498. Caulton, K. G.; Chisholm, M. H.; Drake, S. R.; Folting, K. *J. Chem. Soc., Chem. Comm.* **1990**, 1349. Cloke, F. G. N.; Hitchcock, P. B.; Lappert, M. F.; Lawless, G. A.; Royo, B. *J. Chem. Soc., Chem. Comm.* **1991**, 724. (b) For diketonates, see, for example: Prasad, R. N.; Jindal, M.; Sharma, M. *Revue Roumaine De Chimie* **1994**, *39*, 65. Nichiporuk, R. V.; Pechurova, N. I.; Snezhko, N. I.; Martynenko, L. I.; Kaul, A. R.; Zainina, A. S.; Shergina, S. I.; Sokolov, I. E. *Zh. Neorg. Khim.* **1991**, *36*, 2279. Hashimoto, T.; Kitazawa, K.; Nakabayashi, M.; Shiraishi, T.; Suemune, Y.; Yamamoto, T.; Koinuma, H. *Appl. Organomet. Chem.* **1991**, *5*, 325. Turnipseed, S. B.; Barkley, R. M.; Sievers, R. E. *Inorg. Chem.* **1991**, *30*, 1164. Neumayer, D. A.; Studebaker, D. B.; Hinds, B. J.; Stern, C. L.; Marks, T. J. *Chem. Mater.* **1994**, *6*, 878. Chern, C. S.; Liang, S.; Shi, Z. Q.; Yoon, S.; Safari, A.; Lu, P.; Kear, B. H.; Goodreau, B. H.; Marks, T. J.; Hou, S. Y. *Appl. Phys. Lett.* **1994**, *64*, 3181. Han, B.; Neumayer, D. A.; Goodreau, B. H.; Marks, T. J.; Zhang, H.; Dravid, V. P. *Chem. Mater.* **1994**, *6*, 18. Buriak, J. M.; Cheatham, L. K.; Gordon, R. G.; Graham, J. J.; Barron, A. R. *Eur. J. Solid State Inorg. Chem.* **1992**, *29*, 43.
- (2) Irgolic, K. J. *The Organic Chemistry of Tellurium*; Gordon and Breach: New York, 1974.

- (3) Haller, W. S.; Irgolic, K. J. *J. Organomet. Chem.* **1972**, *38*, 97.  
 (4) Petraghani, N. *Chem. Ber.* **1963**, *96*, 247.  
 (5) Petraghani, N.; de Moura Campos, M. *Chem. Ber.* **1963**, *96*, 249.  
 (6) Gysling, H. J. In *The Chemistry of Organic Selenium and Tellurium Compounds*; Patai, S. Rappoport, Z., Ed.; Wiley: New York, 1986; Vol. 1, p 679.  
 (7) Bonasia, P. J.; Gindelberger, D. E.; Dabbousi, B. O.; Arnold, J. J. *Am. Chem. Soc.* **1992**, *114*, 5209.  
 (8) Bonasia, P. J.; Christou, V.; Arnold, J. J. *Am. Chem. Soc.* **1993**, *115*, 6777.  
 (9) Gindelberger, D. E.; Arnold, J. J. *Am. Chem. Soc.* **1992**, *114*, 6242.  
 (10) Becker, G.; Klinkhammer, K. W.; Schwarz, W.; Westerhausen, M.; Hildenbrand, T. Z. *Naturforsch.* **1992**, *47b*, 1225.

Scheme 1

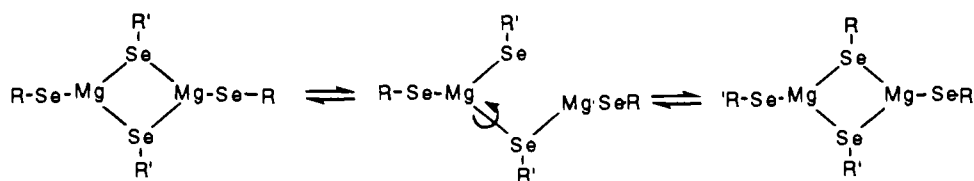
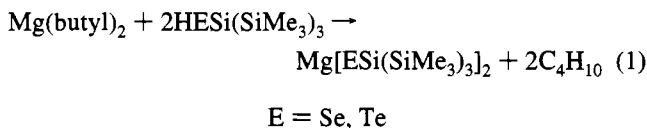


Table 1. Physical Data for New Compounds

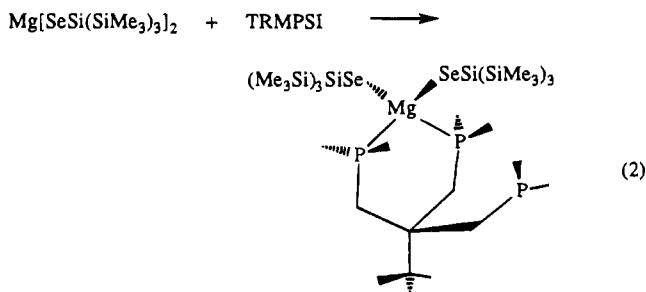
compd	% yield	mp/°C	color
Mg[SeSi(SiMe <sub>3</sub> ) <sub>3</sub> ] <sub>2</sub>	71	239–241	colorless
Mg[TeSi(SiMe <sub>3</sub> ) <sub>3</sub> ] <sub>2</sub>	77	222–227	lt. yellow
Mg[SeSi(SiMe <sub>3</sub> ) <sub>3</sub> ] <sub>2</sub> (TRMPSI)	73	197–199	colorless
Mg[TeSi(SiMe <sub>3</sub> ) <sub>3</sub> ] <sub>2</sub> (THF) <sub>2</sub>	68	>300	yellow
Mg[TeSi(SiMe <sub>3</sub> ) <sub>3</sub> ] <sub>2</sub> (pyridine) <sub>2</sub>	73	>300	yellow
Mg[12-crown-4] <sub>2</sub> [TeSi(SiMe <sub>3</sub> ) <sub>3</sub> ] <sub>2</sub>	50	215–216 d	orange
Ca[SeSi(SiMe <sub>3</sub> ) <sub>3</sub> ] <sub>2</sub> (TMEDA) <sub>2</sub>	64	217–219	colorless
Ca[TeSi(SiMe <sub>3</sub> ) <sub>3</sub> ] <sub>2</sub> (THF) <sub>4</sub>	46	261–262	yellow
Ca[TeSi(SiMe <sub>3</sub> ) <sub>3</sub> ] <sub>2</sub> (pyridine) <sub>4</sub>	66	>300	yellow
Sr[SeSi(SiMe <sub>3</sub> ) <sub>3</sub> ] <sub>2</sub> (TMEDA) <sub>2</sub>	63	208–210	colorless
Sr[TeSi(SiMe <sub>3</sub> ) <sub>3</sub> ] <sub>2</sub> (THF) <sub>4</sub>	25	>300	yellow
Sr[TeSi(SiMe <sub>3</sub> ) <sub>3</sub> ] <sub>2</sub> (pyridine) <sub>4</sub>	75	>300	yellow
Ba[SeSi(SiMe <sub>3</sub> ) <sub>3</sub> ] <sub>2</sub> (TMEDA) <sub>2</sub>	69	285–286	lt. yellow
Ba[TeSi(SiMe <sub>3</sub> ) <sub>3</sub> ] <sub>2</sub> (THF) <sub>4</sub>	52	>300	yellow
Ba[TeSi(SiMe <sub>3</sub> ) <sub>3</sub> ] <sub>2</sub> (pyridine) <sub>5</sub>	73	162–165	yellow

the lithium chalcogenolate (THF)<sub>2</sub>LiESi(SiMe<sub>3</sub>)<sub>3</sub> and group 2 dihalides were unsuccessful as they generally led to intractable mixtures. In contrast, chalcogenolysis<sup>7,8</sup> of compounds containing metal–nitrogen or metal–carbon bonds afforded an extremely clean and simple route to the metal chalcogenolates. For example, eq 1 shows the chalcogenolysis of dibutylmagnesium



nesium in hexane, which gave the homoleptic selenolate and tellurolate in good yield. Table 1 lists yields and physical data for all new compounds. The magnesium chalcogenolates are all oxygen- and moisture-sensitive, pale-colored crystalline solids that are generally quite soluble in hydrocarbon and ether solvents. When stored under dry nitrogen at room temperature, the compounds are stable indefinitely.

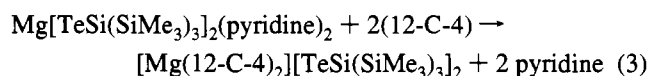
The homoleptic magnesium selenolate reacted with the potentially tridentate base TRMPSI to form Mg[SeSi(SiMe<sub>3</sub>)<sub>3</sub>]<sub>2</sub>(TRMPSI), which was isolated as a colorless crystalline solid (eq 2). In solution and in the solid-state, the Mg is four-coordinate with two arms of the phosphine bound and one free, as determined by multinuclear NMR and X-ray studies (see below).



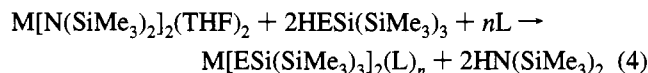
Lewis donor adducts Mg[TeSi(SiMe<sub>3</sub>)<sub>3</sub>]<sub>2</sub>L<sub>2</sub> (L = THF, pyridine) were prepared by recrystallization of Mg[TeSi(SiMe<sub>3</sub>)<sub>3</sub>]<sub>2</sub> in the presence of the Lewis base. The THF compound was also isolated following the reaction of Hg[TeSi-

(SiMe<sub>3</sub>)<sub>3</sub>]<sub>2</sub><sup>11</sup> with an excess of magnesium powder in THF. The X-ray crystal structure of Mg[TeSi(SiMe<sub>3</sub>)<sub>3</sub>]<sub>2</sub>(THF)<sub>2</sub> is discussed below.

Treatment of the magnesium tellurolate with 12-crown-4 results in displacement of both the pyridine and the tellurolate ligands to form the ionic complex shown in eq 3. Crystals of the 2:1 salt ( $\Lambda_m = 200 \Omega^{-1} \text{ cm}^2 \text{ mol}^{-1}$ ; 0.1 M MeCN<sup>12</sup>) were obtained as pale yellow plates from THF.



**Ca, Sr, and Ba Derivatives.** Reactions of the bis(trimethylsilylamide) complexes of Ca, Sr and Ba<sup>13</sup> and 2 equiv of HESi(SiMe<sub>3</sub>)<sub>3</sub> (E = Se, Te)<sup>7,8</sup> in hexane gave high yields of the selenolates and tellurolates, which were isolated as various Lewis-base adducts (eq 4).



M = Ca, Sr, Ba; E = Se, Te; L = TMEDA, THF, pyridine

The selenolate complexes of Ca, Sr, and Ba were isolated as bis-TMEDA adducts as evidenced by NMR spectroscopy and, in the case of Sr[SeSi(SiMe<sub>3</sub>)<sub>3</sub>]<sub>2</sub>(TMEDA)<sub>2</sub>, by X-ray crystallography (see below).

The tellurolate complexes were isolated as both THF and pyridine adducts. At room temperature, the THF complexes slowly lose coordinated solvent, but they are otherwise stable to heat, normal room light, and can be kept under nitrogen for prolonged periods. The analogous pyridine adducts were prepared by recrystallization of the THF complexes from pyridine, or by the addition of pyridine to reaction mixtures.

The selenolates are all colorless or light yellow crystalline solids that dissolve, at least sparingly, in hydrocarbons. The magnesium derivatives are more soluble than the heavier group 2 TMEDA derivatives.<sup>14,15</sup> These materials are not as air-sensitive as the tellurolate derivatives, but they decompose to the diselenide on exposure to air.

The tellurolates are yellow crystalline, air-sensitive materials with high melting points. Dissolution in hydrocarbon and ethereal solvents affords solutions that are stable indefinitely, although they react with O<sub>2</sub> and water to form the tellurol and ditelluride, respectively.

**NMR Spectroscopic Studies.** Although the solid-state structures of the homoleptic magnesium chalcogenolates are presently unknown, we obtained NMR data that indicates the magnesium selenolate is a stereochemically nonrigid dimer in solution. At room temperature a single peak is observed in the <sup>1</sup>H NMR spectrum in toluene-*d*<sub>8</sub>. The signal broadens, then

(11) Bonasia, P. J.; Arnold, J. *Inorg. Chem.* **1992**, *31*, 2508.

(12) Geary, W. J. *Coord. Chem. Rev.* **1971**, *7*, 81.

(13) Bradley, D. C.; Hursthouse, M. B.; Ibrahim, A. A.; Malik, K. M. A.; Motevalli, M.; Mösel, R.; Powell, H.; Runnacles, J. D.; Sullivan, A. C. *Polyhedron* **1990**, *9*, 2959.

(14) Gindelberger, D. E.; Arnold, J. *Inorg. Chem.* **1993**, *32*, 5813.

(15) Cary, D. R.; Arnold, J. *Inorg. Chem.* **1994**, *33*, 1791.

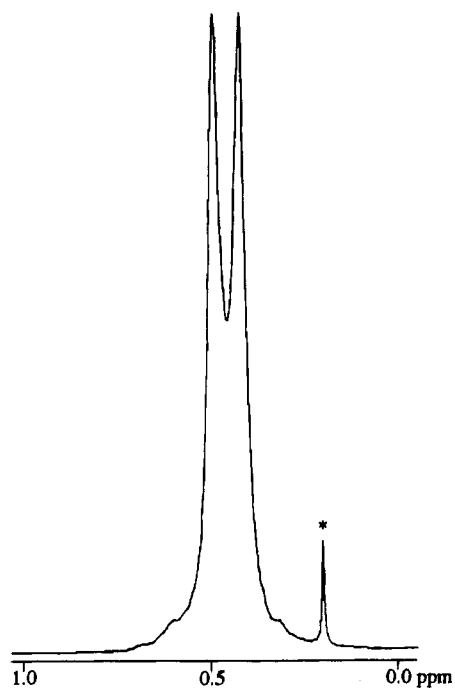


**Figure 1.**  $^1\text{H}$  NMR spectrum of  $\text{Mg}[\text{SeSi}(\text{SiMe}_3)_3]_2$  at  $-88\text{ }^\circ\text{C}$ . (The starred peak is due to co-crystallized HMDSO.)

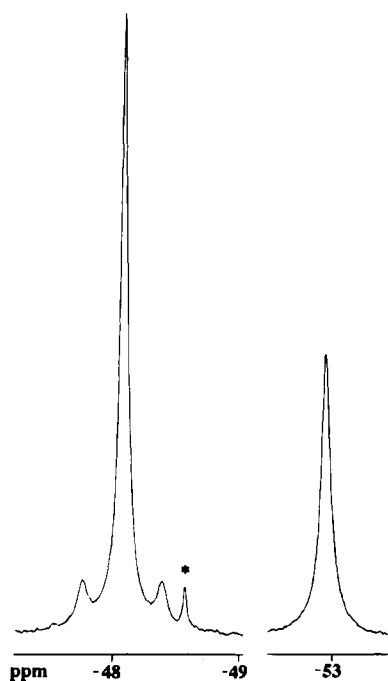


**Figure 2.**  $^{31}\text{P}$  NMR spectrum of  $\text{Mg}[\text{SeSi}(\text{SiMe}_3)_3]_2(\text{TRMPSI})$  at  $-90\text{ }^\circ\text{C}$ . (The starred peak is an unidentified impurity.)

splits into two on cooling to  $-88\text{ }^\circ\text{C}$  as shown in Figure 1. This behavior is consistent with an intramolecular exchange of bridging and terminal ligands in a dimeric structure that is slow on the NMR time-scale at low temperature (Scheme 1). An alternative intermolecular exchange process is not considered likely since the coalescence behavior is concentration independent. The homoleptic tellurolate behaves similarly except here the exchange process could not be frozen out, even on cooling to  $-90\text{ }^\circ\text{C}$ . Overall, the behavior of the Mg derivatives is analogous to that observed in the Group 12 derivatives  $\text{M}[\text{TeSi}(\text{SiMe}_3)_3]_2$  ( $\text{M} = \text{Zn}, \text{Cd}$ ) although the rates of exchange are much slower in the latter.<sup>11</sup>

The TRMPSI derivative  $\text{Mg}[\text{SeSi}(\text{SiMe}_3)_3]_2(\text{TRMPSI})$  is also fluxional in solution. At room temperature,  $^1\text{H}$  NMR spectroscopy

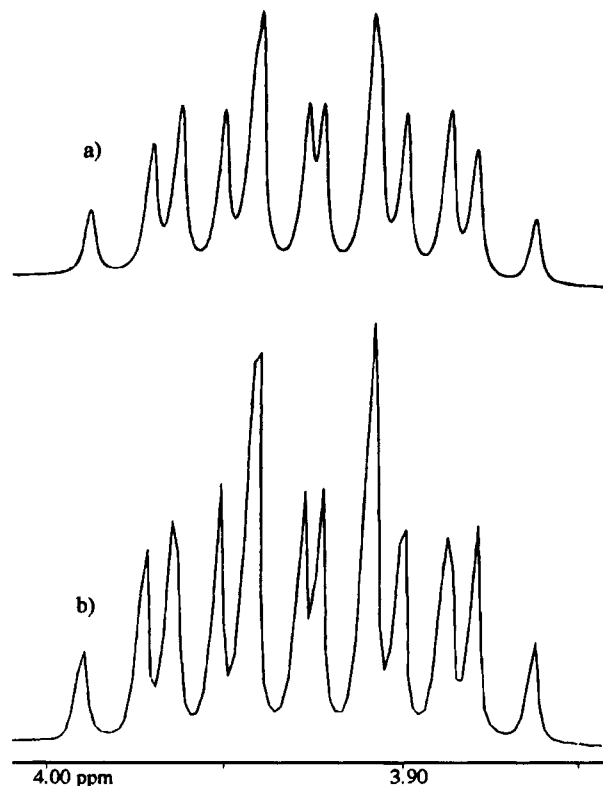


**Figure 3.** Calculated (a) and observed (b)  $^1\text{H}$  NMR resonances for the 12-C-4 protons in  $\text{Mg}[\text{TeSi}(\text{SiMe}_3)_3]_2(12\text{-C-4})_2$ .

copy shows equivalent selenolates and a broad resonance in the  $^{31}\text{P}$  NMR spectrum. On cooling to  $-90\text{ }^\circ\text{C}$ , the proton spectrum broadens and the phosphorus spectrum sharpens and splits into two signals (Figure 2). Selenium satellites on the more intense signal identifies this as arising from the two bound arms of the TRMPSI ligand while the remaining peak is assigned to the free  $-\text{PMe}_2$  group. Thus, the low temperature spectrum is in accordance with the solid state structure described below.

The room temperature  $^1\text{H}$  NMR spectrum of  $\text{Mg}[\text{TeSi}(\text{SiMe}_3)_3]_2(12\text{-C-4})_2$  at 400 MHz consists of a singlet for the  $-\text{TeSi}(\text{SiMe}_3)_3$  groups and a complex AA'BB' pattern centered at 3.92 ppm for the ethylenes of the 12-C-4 ligands. Simulation of the latter signal was possible using one geminal ( $J_{\text{AB}} = -11.5$  Hz) and two vicinal couplings ( $J_{\text{AA}'} = J_{\text{BB}'} = 6.6$  Hz,  $J_{\text{AB}'} = 3.9$  Hz) for the inequivalent ethylene protons. The calculated and observed spectra are given in Figure 3.<sup>16</sup> These results show that the cation has a rigid structure, i.e. that no exchange of 12-C-4 ligands is occurring. Unfortunately we were unable to obtain diffraction-quality crystals and no comparable structures have been reported.

The Ca, Sr, and Ba selenolates displayed straightforward, unremarkable  $^1\text{H}$  NMR spectra. No  $^{77}\text{Se}$  NMR resonances were observed for the TMEDA adducts, perhaps due to their relatively low solubility. The tellurolate pyridine adducts showed singlets in their  $^{125}\text{Te}$  NMR spectra in the narrow range from  $-1578$  to  $-1405$  ppm. The small shift to lower field down this homologous series of main-group metal derivatives contrasts markedly with the ranges seen for d-metal complexes. For example,  $^{125}\text{Te}$  shifts in the series of Group 4 tellurolates  $\text{Cp}_2\text{M}[\text{TeSiPh}_3]_2$  move substantially *upfield*, from 709 to  $-170$ , as the group is descended from Ti to Hf.<sup>17</sup>

(16) Marat, K.; Sebastian, R. A. *NMR Spectral Simulation and Analysis Package X-11*, ver. 940101, Univ. of Manitoba, Winnipeg, 1994.

(17) Gindelberger, D. E.; Arnold, J. *Organometallics*, in press.

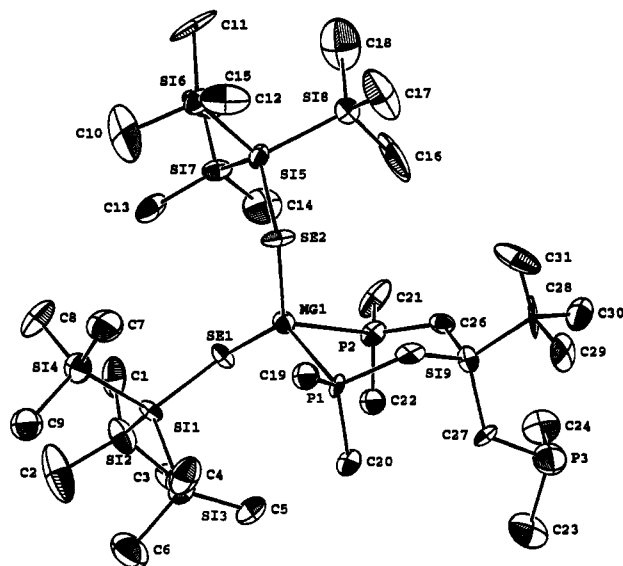


Figure 4. ORTEP view of  $\text{Mg}[\text{SeSi}(\text{SiMe}_3)_3]_2(\text{TRMPSI})$ .

**X-ray Structures of Selenolate Derivatives.** A view of the solid-state structure of  $\text{Mg}[\text{SeSi}(\text{SiMe}_3)_3]_2(\text{TRMPSI})$  is shown in Figure 4. The metal is bound to the two selenolates and two  $\text{PMe}_2$  groups of the TRMPSI ligand, with no close contacts between molecules in the unit cell. Structural data reported for TRMPSI<sup>18–20</sup> and closely related phosphines<sup>21–24</sup> show that tridentate coordination is preferred; the reluctance of the third phosphorus to chelate in our case is undoubtedly a steric effect. At 2.65(1) and 2.66(1) Å, the Mg–P bond lengths are consistent with the predicted covalent value (2.65 Å<sup>25</sup>) but are longer than that found in the only other compound with a Mg–P interaction, the phosphide (TMEDA) $\text{Mg}[\text{PPh}]_2$  (2.591 Å average).<sup>26</sup> The difference between the two structurally characterized molecules is, nonetheless, in line with that expected between four- and three-coordinate phosphorus, respectively. The Mg–Se distances (2.483, 2.500 Å; Table 3) are in the range predicted based on covalent radii (2.46 Å).<sup>25</sup> The two Se–Mg–P angles are noticeably different, probably as a result of simple interligand repulsion. The angle between the planes defined by P1–Mg1–P2 and Se1–Mg1–Se2 (66.7(3)°) is far less than expected for tetrahedral coordination; however this type of distortion is not uncommon, having been observed in related 4-coordinate chalcogenolate species.<sup>11,14</sup> As in all the structures described here, parameters associated with the Si–(SiMe<sub>3</sub>)<sub>3</sub> group are similar to related derivatives and are otherwise unremarkable.

The molecular structure of  $\text{Sr}[\text{SeSi}(\text{SiMe}_3)_3]_2(\text{TMEDA})_2$  is shown as an ORTEP diagram in Figure 5. The molecule is coordinated in a pseudo-octahedral fashion in a similar manner to that found in  $\text{Yb}[\text{Se}(\text{Si}(\text{SiMe}_3)_3)]_2(\text{TMEDA})_2$  with the metal

lying on a crystallographic inversion center. The Sr–Se bond (2.946(1) Å; Table 4) is slightly shorter than would be expected based on covalent radii (3.08 Å).<sup>25</sup> The Sr–N distances are shorter than found in the related eight-coordinate strontium derivative  $[\text{Sr}(\text{ethylenediamine})_4]_2(\text{As}_3\text{Se}_6)\text{Cl}$  (2.743 Å average),<sup>27</sup> as expected based on the difference in coordination numbers. The three trans interactions are 180° as required by the inversion symmetry, and the Sr–Se–Si angle is also close to linear. Structures of related tellurolates show much more acute angles at the chalcogen (M–Te–Si, 97.4–133.8°). It is possible that the large Sr–Se–Si angle is due to the proximity of the silyl group to the metal center. Relative to the tellurolate complexes, the silyl group is closer to the metal and would therefore interact more with ancillary ligands forcing a larger angle at Se.

**X-ray Structures of Tellurolate Derivatives.** The X-ray structure of  $\text{Mg}[\text{TeSi}(\text{SiMe}_3)_3]_2(\text{THF})_2$  shows the pseudo-tetrahedral metal surrounded by two THF oxygens and two tellurolate ligands (Figure 6). The Mg–Te bond lengths (Table 5) are virtually identical (2.720, 2.714 (1) Å) and are only slightly longer than values predicted by covalent radii (2.66 Å).<sup>25</sup> The Mg–O bond lengths (2.035, 2.038 Å) are similar to those found in known tetrahedral Mg–THF adducts which lie in the range 2.002–2.110 Å.<sup>13,28–30</sup> As with similar structures incorporating this ligand<sup>11,14</sup> steric bulk is no doubt responsible for the large Te–Mg–Te angle of 135.48(4)° and the rather acute O–Mg–O angle of 94.8(1)°. The Te–Mg–O angles are not equal, so that for each of the two tellurium atoms there is one large and one small. This difference may be attributed to steric repulsion from the tellurium sp<sup>3</sup> lone pairs, since the smaller angle appears when the THF oxygen is trans to the Te–Si vector in the tellurolate ligand, but packing effects cannot be excluded.

The structure of  $\text{Ca}[\text{TeSi}(\text{SiMe}_3)_3]_2(\text{THF})_4$  features a distorted octahedral coordination sphere about the metal. Figure 7 shows an ORTEP view of the molecule illustrating the disordered THF. Following our preliminary account of this structure,<sup>9</sup> another report describing a structural study of the same molecule appeared.<sup>10</sup> These two determinations are identical within experimental error. The molecule has strict inversion symmetry, with the calcium at the origin of the cell. Inspection of the angles between cis-coordination sites highlights the extent to which the molecule is distorted. These angles (Table 6), which range from 77.33(5)° to 92.73(9)°, appear to result from interligand repulsions attributable to the bulk of the tellurolate group. The estimated length of a Ca–Te covalent bond (3.10 Å<sup>25</sup>) is shorter than the experimentally determined value of 3.197(1) Å.

The structure of  $\text{Ba}[\text{TeSi}(\text{SiMe}_3)_3]_2(\text{pyridine})_5$  is shown in Figure 8. It crystallizes with five pyridine ligands about its equatorial plane and two axial tellurolates. The molecule possesses a crystallographic 2-fold axis which runs through one of the pyridine ligands (N1) and the Ba atom. The Ba–Te bond length (Table 7) is close to that predicted by covalent radii (3.34 Å<sup>25</sup>). The Ba–N2 and Ba–N3 bond lengths (2.888 Å average) are similar to the Ba–N distances in the only other comparable pyridine adduct,  $\text{BaHg}(\text{CN})_4(\text{pyridine})_4$  (2.906, 2.921 Å<sup>31</sup>). The

(18) Gardner, T. G.; Girolami, G. S. *J. Chem. Soc., Chem. Comm.* **1987**, 1758.

(19) Gardner, T. G.; Girolami, G. S. *Organometallics* **1987**, *6*, 2551.

(20) Gardner, T. G.; Girolami, G. S. *Angew. Chem., Int. Ed. Engl.* **1988**, *27*, 1693.

(21) Boncella, J. M.; Green, M. L. H.; O'Hare, D. *J. Chem. Soc., Chem. Comm.* **1986**, 618.

(22) Boncella, J. M.; Green, M. L. H. *J. Organomet. Chem.* **1987**, *217*, 325.

(23) Green, M. L. H.; O'Hare, D.; Watkin, J. G. *J. Chem. Soc., Chem. Commun.* **1989**, 698.

(24) Dahlenburg, I.; Kerstan, S.; Werner, D. *J. Organomet. Chem.* **1991**, *411*, 457.

(25) Porterfield, W. W. *Inorganic Chemistry: A Unified Approach*, 2nd ed.; Academic Press: San Diego, CA, 1993.

(26) Hey, E.; Englehardt, L. M.; Raston, C. L.; White, A. H. *Angew. Chem., Int. Ed. Engl.* **1987**, *26*, 81.

(27) Sheldrick, W. S.; Kaub, J. Z. *Naturforsch.* **1985**, *40b*, 1022.

(28) Del Piero, G.; Cesari, M.; Cucinella, S.; Mazzei, A. *J. Organomet. Chem.* **1977**, *137*, 265.

(29) Markies, P. R.; Schat, G.; Akkerman, O. S.; Bickelhaupt, F.; Smeets, W. J. J.; Van der Sluis, P.; Speck, A. L. *J. Organomet. Chem.* **1990**, *393*, 315.

(30) Waggoner, K. M.; Power, P. P. *Organometallics* **1992**, *11*, 3209.

(31) Brodersen, K.; Beck, I.; Beck, R.; Hummel, H. U.; Liehr, G. Z. *Anorg. Allg. Chem.* **1984**, *516*, 30.

Table 2. Summary of X-ray Diffraction Data

	compound				
	Mg[SeSi(SiMe <sub>3</sub> ) <sub>3</sub> ] <sub>2</sub> - (TRMPPI)	Sr[SeSi(SiMe <sub>3</sub> ) <sub>3</sub> ] <sub>2</sub> - (TMEDA) <sub>2</sub>	Mg[TeSi(SiMe <sub>3</sub> ) <sub>3</sub> ] <sub>2</sub> - (THF) <sub>2</sub>	Ca[TeSi(SiMe <sub>3</sub> ) <sub>3</sub> ] <sub>2</sub> - (THF) <sub>4</sub>	Ba[TeSi(SiMe <sub>3</sub> ) <sub>3</sub> ] <sub>2</sub> - (pyridine) <sub>5</sub>
formula	C <sub>31</sub> H <sub>87</sub> MgSi <sub>9</sub> P <sub>3</sub> Se <sub>2</sub>	C <sub>30</sub> H <sub>86</sub> N <sub>4</sub> Si <sub>8</sub> Se <sub>2</sub> Sr	C <sub>26</sub> H <sub>70</sub> O <sub>2</sub> Si <sub>8</sub> MgTe <sub>2</sub>	C <sub>34</sub> H <sub>86</sub> O <sub>4</sub> Si <sub>8</sub> CaTe <sub>2</sub>	C <sub>43</sub> H <sub>79</sub> N <sub>5</sub> Si <sub>8</sub> Te <sub>2</sub> Ba
mol wt	987.9	972.9	919.0	1079.0	1283.4
T/°C	-128	-108	-85	-88	-103
space group	P2 <sub>1</sub> /n	P2 <sub>1</sub> /c	P1	P1	C2/c
a/Å	13.905(7)	9.388(3)	12.033(1)	9.965(2)	13.630(2)
b/Å	15.975(5)	12.322(4)	12.650(2)	13.822(3)	15.933(2)
c/Å	25.55(1)	23.65(1)	16.757(3)	10.434(1)	30.363(4)
α/deg	90.0	90.0	98.88(1)	87.15(1)	90.0
β/deg	91.77(3)	95.91(3)	104.85(1)	86.01(1)	97.41(1)
γ/deg	90.0	90.0	95.16(1)	89.96(1)	90.0
vol/Å <sup>3</sup>	5674(6)	2724(3)	2413(1)	1432.0(7)	6538(2)
Z	4	4	2	1	4
d <sub>calcd</sub> (g cm <sup>-3</sup> )	1.156	2.373	1.26	1.25	1.30
cryst size/mm	0.30 × 0.15 × 0.15	0.28 × 0.20 × 0.15	0.20 × 0.42 × 0.45	0.30 × 0.40 × 0.40	0.22 × 0.25 × 0.38
scan mode	ω	ω	θ-2θ	θ-2θ	ω
2θ range/deg	3-45	3-45	3-45	3-55	3-50
collcn range	+h,+k,±l	+h,+k,±l	+h,+k,±l	+h,+k,±l	+h,+k,±l
abs coeff/cm <sup>-1</sup>	15.9	49.5	14.4	13.0	16.6
no. unique refls	6640	3556	6281	6549	5751
refls w. F <sup>2</sup> > 3σ(F <sup>2</sup> )	2110	1739	5519	5377	3674
final R, R <sub>w</sub>	0.0784, 0.0630	0.0484, 0.0439	0.0254, 0.0329	0.0332, 0.0439	0.0293, 0.0316

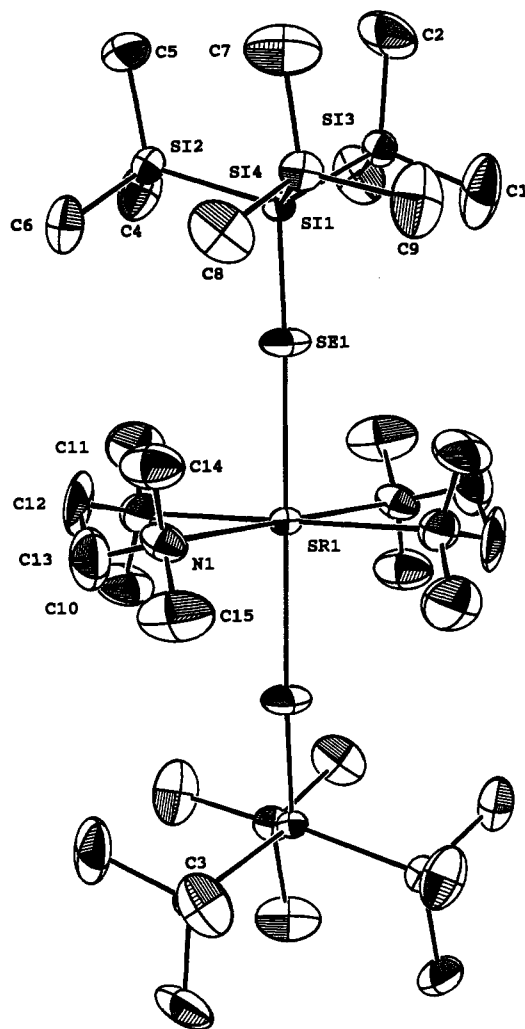
Table 3. Selected Metrical Parameters for Mg[SeSi(SiMe<sub>3</sub>)<sub>3</sub>]<sub>2</sub>(TRMPPI)

Bond Distances (Å)			
Mg1-Se1	2.483(8)	Mg1-P2	2.66(1)
Mg1-Se2	2.500(8)	Se1-Si1	2.266(7)
Mg1-P1	2.65(1)	Se2-Si5	2.300(7)
Bond Angles (deg)			
Se1-Mg1-P1	127.4(4)	Se1-Mg1-Se2	132.7(3)
Se1-Mg1-P2	93.1(3)	P1-Mg1-P2	87.9(3)
Se2-Mg1-P1	90.4(3)	Mg1-Se1-Si1	115.5(3)
Se2-Mg1-P2	118.5(4)	Mg1-Se2-Si5	113.5(3)

plane defined by N2-Ba-N2 is bent relative to the plane defined by N1-Ba-N3 and appears to be the result of steric interaction between the pyridine ligands and the silyl groups. The silyl groups are bent toward the equatorial ligands, and the N2 pyridines move out of the equatorial plane to minimize interaction. The Te-Ba-Te angle is slightly less than 180° and might be a result of either interactions with the pyridine ligands or packing effects.

### Experimental Section

Inert atmosphere glovebox and Schlenk-line techniques were used throughout the preparative procedures. Full details of our standard operating procedures were given earlier.<sup>14</sup> Hexamethyldisiloxane (HMDSO) was distilled from sodium, under nitrogen. Diethyl ether, hexanes, benzene, pentane and toluene were all predried over 4 Å molecular sieves and, with the exception of toluene, were all distilled from purple sodium/benzophenone under N<sub>2</sub>. Toluene was distilled from sodium under N<sub>2</sub>. All NMR solvents were dried like their undeuterated counterparts, but were purified by vacuum transfer. The compounds M[N(SiMe<sub>3</sub>)<sub>2</sub>]<sub>2</sub>(THF)<sub>2</sub> (M = Ca, Sr, Ba),<sup>13</sup> HESi(SiMe<sub>3</sub>)<sub>3</sub> (E = Se, Te),<sup>7,8</sup> and TRMPPI<sup>32</sup> were made by literature procedures. Dibutylmagnesium (1.07 M in heptane, Aldrich) was used as received. Melting points were determined in sealed capillaries under nitrogen and are uncorrected. IR spectra were recorded as Nujol mulls between KBr plates. Chemical shifts (δ) for <sup>1</sup>H NMR spectra are relative to residual protium in the deuterated solvents listed (e.g. C<sub>6</sub>D<sub>6</sub>, δ 7.15 ppm). Chemical shifts for <sup>125</sup>Te NMR spectra are relative to TeMe<sub>2</sub> at 0 ppm by reference to external Te(OH)<sub>6</sub> in D<sub>2</sub>O (1.74M) at δ 712 ppm, and were performed at ambient temperatures in 5 mL tubes at 94.5726 MHz. Elemental analyses and EI/MS measurements were performed within the College of Chemistry, University of California, Berkeley, CA.

Figure 5. ORTEP view of Sr[SeSi(SiMe<sub>3</sub>)<sub>3</sub>]<sub>2</sub>(TMEDA)<sub>2</sub>.

**General Synthetic Method for Preparation of M[ESi(SiMe<sub>3</sub>)<sub>3</sub>]<sub>2</sub>(L)<sub>n</sub>.** Unless noted otherwise, the compounds described below were prepared by addition of ca. 1 mmol of either MgBu<sub>2</sub> or M[N(SiMe<sub>3</sub>)<sub>2</sub>]<sub>2</sub>(THF)<sub>2</sub> (M = Ca, Sr, Ba) dissolved in hexanes (20 mL) to 2 equiv of HESi(SiMe<sub>3</sub>)<sub>3</sub> (E = Se, Te) in hexanes (20 mL). After stirring for 1 h, the volatiles were evaporated under vacuum and the compounds were

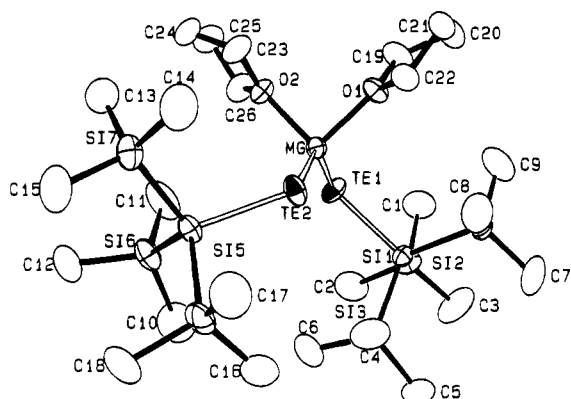


Figure 6. ORTEP view of  $\text{Mg}[\text{TeSi}(\text{SiMe}_3)_2]_2(\text{THF})_2$ .

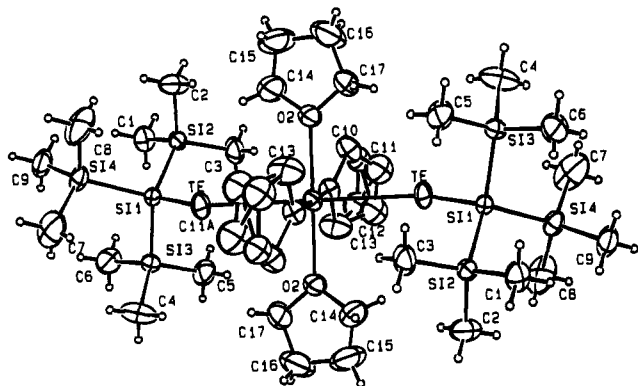


Figure 7. ORTEP view of  $\text{Ca}[\text{TeSi}(\text{SiMe}_3)_2]_2(\text{THF})_4$ .

Table 4. Selected Metrical Parameters for  $\text{Sr}[\text{SeSi}(\text{SiMe}_3)_2]_2(\text{TMEDA})_2$

Bond Distances (Å)			
Sr1-Se1	2.946(1)	Sr1-N2	2.69(1)
Sr1-N1	2.69(1)	Se1-Si1	2.235(3)
Bond Angles (deg)			
Se1-Sr1-N1	93.8(2)	Sr-Se1-Si1	167.02(9)
Se1-Sr1-N2	88.5(3)	N1-Sr1-N2	70.0(3)

Table 5. Selected Metrical Parameters for  $\text{Mg}[\text{TeSi}(\text{SiMe}_3)_2]_2(\text{THF})_2$

Bond Distances (Å)			
Mg-Te1	2.720(1)	Mg-O2	2.038(2)
Mg-Te2	2.714(1)	Te1-Si1	2.504(1)
Mg-O1	2.035(2)	Te2-Si5	2.504(1)
Bond Angles (deg)			
Te1-Mg-O1	117.77(7)	Te1-Mg-Te2	135.48(4)
Te1-Mg-O2	96.37(7)	O1-Mg-O2	94.7(1)
Te2-Mg-O1	97.51(7)	Mg-Te1-Si1	113.36(3)
Te2-Mg-O2	114.37(7)	Mg-Te2-Si5	115.31(3)

purified by crystallization from the solvents indicated. The donor adducts were prepared similarly, but with the addition of a slight excess of the Lewis base.

**Mg[SeSi(SiMe<sub>3</sub>)<sub>2</sub>]<sub>2</sub>.** Colorless crystals were obtained from HMDSO (71%). Mp: 239–241 °C. <sup>1</sup>H NMR (300 MHz, C<sub>6</sub>D<sub>6</sub>): δ 0.40 (s). IR: 1377 m, 1310 w, 1058 w, 861 sh, 836 s, 743 w, 688 s, 622 s cm<sup>-1</sup>. Anal. Calcd for C<sub>18</sub>H<sub>54</sub>MgSi<sub>8</sub>Se<sub>2</sub>: C, 31.9; H, 8.03. Found: C, 32.1; H, 8.08.

**Mg[TeSi(SiMe<sub>3</sub>)<sub>2</sub>]<sub>2</sub>.** Pale yellow crystals were obtained from hexanes (77%). Mp: 222–227 °C. <sup>1</sup>H NMR (400 MHz, C<sub>6</sub>D<sub>6</sub>): δ 0.44 (s). IR: 1243 m, 835 s, 688 m, 626 m cm<sup>-1</sup>. Anal. Calcd for C<sub>18</sub>H<sub>54</sub>MgSi<sub>8</sub>Te<sub>2</sub>: C, 27.9; H, 7.02. Found: C, 27.8; H, 6.50.

**Mg[SeSi(SiMe<sub>3</sub>)<sub>2</sub>]<sub>2</sub>[TRMPSI].** Colorless crystals were obtained from hexanes (73%). Mp: 197–199 °C. <sup>1</sup>H NMR (300 MHz, C<sub>6</sub>D<sub>6</sub>): δ 1.08 (s, 18 H), 0.91 (s, 9 H), 0.83 (s, 6 H), 0.43 (s, 54 H). IR: 1297

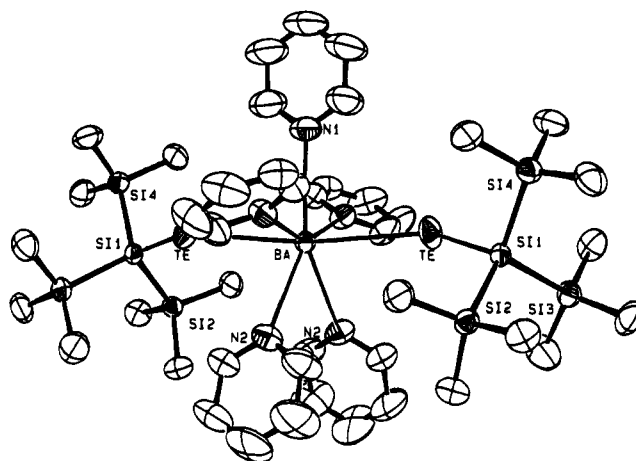


Figure 8. ORTEP view of  $\text{Ba}[\text{TeSi}(\text{SiMe}_3)_2]_2(\text{pyridine})_5$ .

Table 6. Selected Metrical Parameters for  $\text{Ca}[\text{TeSi}(\text{SiMe}_3)_2]_2(\text{THF})_4$

Bond Distances (Å)			
Ca-Te	3.197(1)	Ca-O2	2.410(2)
Ca-O1	2.363(2)	Te-Si1	2.483(1)
Bond Angles (deg)			
Te-Ca-O1	77.33(5)	Ca-Te-Si1	128.54(2)
Te-Ca-O1'	102.67(5)	O1-Ca-O2	87.27(9)
Te-Ca-O2	89.00(6)	O1-Ca-O2'	92.73(9)
Te-Ca-O2'	91.00(6)		

Table 7. Selected Metrical Parameters for  $\text{Ba}[\text{TeSi}(\text{SiMe}_3)_2]_2(\text{pyridine})_5$

Bond Distances (Å)			
Ba-Te	3.382(1)	Ba-N3	2.874(3)
Ba-N1	2.934(5)	Te-Si	2.467(1)
Ba-N2	2.856(4)		
Bond Angles (deg)			
Te-Ba-Te'	171.91(2)	Te-Ba-N1	85.95(1)
Ba-Te1-Si1	144.42(3)	Te-Ba-N2	103.63(9)
N2-Ba-N2'	67.0(1)	Te-Ba-N3	85.17(8)
N1-Ba-N3	75.79(7)	Te'-Ba-N2	83.22(9)
N2-Ba-N3	71.7(1)	Te'-Ba-N3	92.84(8)

m, 1240 s, 1127 m, 1110 w, 1099 w, 1088 m, 1060 w, 1007 w, 952 w, 942 m, 912 s, 891 m, 865 sh, 830 s, 786 sh, 732 m, 721 m, 687 s, 656 w, 623 s cm<sup>-1</sup>. Anal. Calcd for C<sub>31</sub>H<sub>87</sub>MgSi<sub>9</sub>P<sub>3</sub>Se<sub>2</sub>: C, 37.6; H, 8.88. Found: C, 38.0; H, 8.86.

**Mg[TeSi(SiMe<sub>3</sub>)<sub>2</sub>]<sub>2</sub>(THF)<sub>2</sub>.** Method A. A 0.15 g portion of Mg[TeSi(SiMe<sub>3</sub>)<sub>2</sub>] was dissolved in hexanes (10 mL) and THF (3 mL) was added. The volume was reduced to 1 mL and the solution was cooled to -40 °C to give pale yellow crystals of the product (0.12 g, 68%).

Method B. Hg[TeSi(SiMe<sub>3</sub>)<sub>2</sub>]<sub>2</sub><sup>11</sup> (0.70 g, 0.9 mmol) was stirred with Mg powder (0.35 g, 14 mmol) over a period of 30 min. The solvent was removed in vacuo and the residue was recrystallized from hexanes yielding 0.30 g (44%) of product. Mp: >300 °C. <sup>1</sup>H NMR (300 MHz, C<sub>6</sub>D<sub>6</sub>): δ 3.79 (m, 8 H), 1.23 (m, 8 H), 0.50 (s, 54 H). Anal. Calcd for C<sub>18</sub>H<sub>54</sub>MgSi<sub>8</sub>Te<sub>2</sub>: C, 34.0; H, 7.68. Found: C, 33.1; H, 7.67.

**Mg[TeSi(SiMe<sub>3</sub>)<sub>2</sub>]<sub>2</sub>(pyridine)<sub>2</sub>.** Light yellow crystals were obtained from ether (73%). Mp: >300 °C. <sup>1</sup>H NMR (300 MHz, C<sub>6</sub>D<sub>6</sub>): δ 8.86 (d, J 5 Hz, 4 H), 6.79 (t, J 8 Hz, 2H), 6.52 (t, J 6 Hz, 4 H), 0.45 (s, 54 H). <sup>125</sup>Te{<sup>1</sup>H} NMR (C<sub>6</sub>D<sub>6</sub>): δ -1578 (s). Anal. Calcd for C<sub>28</sub>H<sub>64</sub>MgN<sub>2</sub>Si<sub>8</sub>Te<sub>2</sub>: C, 36.1; H, 6.91; N, 3.00. Found: C, 36.3; H, 7.03; N, 2.76.

**Mg[12-crown-4]<sub>2</sub>[TeSi(SiMe<sub>3</sub>)<sub>2</sub>]<sub>2</sub>.** To a solution of Mg[TeSi(SiMe<sub>3</sub>)<sub>2</sub>]<sub>2</sub>(pyridine)<sub>2</sub> (0.30 g, 0.32 mmol) in toluene was added 12-crown-4 (0.11 g, 0.64 mmol). The solution was stirred for 1.5 h and the solvent was removed in vacuo. The pale yellow residue was taken up in THF (100 mL) and filtered. Concentration under vacuum followed by cooling to -40 °C yielded a flaky orange solid (0.18 g,

50%). Mp: 215–216 °C (d).  $^1\text{H}$  NMR (400 MHz,  $\text{CD}_3\text{CN}$ ):  $\delta$  3.92 (m, 32 H), 0.13 (s, 54 H). IR: 1378 m, 1286 w, 1134 w, 1075 s, 1016 m, 939 m, 863 m, 831 s, 731 w, 682 m, 621  $\text{cm}^{-1}$ . Anal. Calcd for  $\text{C}_{34}\text{H}_{86}\text{MgO}_4\text{Si}_8\text{Te}_2$ : C, 36.2; H, 7.69. Found: C, 35.8; H, 7.50.

**Ca[SeSi(SiMe<sub>3</sub>)<sub>3</sub>]<sub>2</sub>(TMEDA)<sub>2</sub>.** An off-white crystalline solid was isolated from hexanes (64%). Mp: 217–219 °C.  $^1\text{H}$  NMR (300 MHz,  $\text{C}_6\text{D}_6$ ):  $\delta$  2.44 (s, 24 H), 2.29 (s, 8 H), 0.38 (s, 54 H). IR: 1377 s, 1300 w, 1290 m, 1186 w, 1162 m, 1126 m, 1071 w, 1027 s, 1015 m, 954 s, 919 w, 865 sh, 833 s, 186 m, 740 w, 685 s, 624 s, 578  $\text{cm}^{-1}$ .

**Ca[TeSi(SiMe<sub>3</sub>)<sub>3</sub>]<sub>2</sub>(THF)<sub>4</sub>.** A light yellow crystalline solid was obtained from THF/hexanes (1:1) (46%). Mp: 261–262 °C.  $^1\text{H}$  NMR (400 MHz,  $\text{C}_6\text{D}_6$ ):  $\delta$  3.97 (m, 16 H), 1.47 (m, 16 H), 0.48 (s, 54 H). Anal. Calcd for  $\text{C}_{34}\text{H}_{86}\text{CaO}_4\text{Si}_8\text{Te}_2$ : C, 37.9; H, 8.03. Found: C, 38.0; H, 7.96.

**Ca[TeSi(SiMe<sub>3</sub>)<sub>3</sub>]<sub>2</sub>(pyridine)<sub>4</sub>.** Large yellow crystals were obtained from ether (66%). Mp: >300 °C.  $^1\text{H}$  NMR (400 MHz,  $\text{C}_6\text{D}_6$ ):  $\delta$  9.51 (d, 8 H), 6.82 (t, 4 H), 6.67 (t, 8 H), 0.42 (s, 54 H).  $^{125}\text{Te}\{^1\text{H}\}$  NMR ( $\text{C}_6\text{D}_6$ ):  $\delta$  -1458 (s). IR: 1622 w, 1596 s, 1572 w, 1488 m, 1442 s, 1377 s, 1306 w, 1252 m, 1235 s, 1225 m, 1152 m, 1070 m, 1034 s, 1002 m, 831 vs, 759 m, 752 m, 700 s, 685 s, 622  $\text{cm}^{-1}$ . Anal. Calcd for  $\text{C}_{38}\text{H}_{74}\text{CaN}_4\text{Si}_8\text{Te}_2$ : C, 41.2; H, 6.74; N, 5.04. Found: C, 41.3; H, 6.72; N, 4.42.

**Sr[SeSi(SiMe<sub>3</sub>)<sub>3</sub>]<sub>2</sub>(TMEDA)<sub>2</sub>.** Colorless crystals were obtained from hexanes (63%). Mp: 208–210 °C.  $^1\text{H}$  NMR (300 MHz,  $\text{C}_6\text{D}_6$ ):  $\delta$  2.37 (s, 24 H), 2.24 (s, 8 H), 0.39 (s, 54 H). IR: 1377 s, 1292 s, 1182 w, 1161 m, 1129 m, 1073 m, 1031 s, 1017 m, 953 m, 865 sh, 835 s, 784 m, 741 w, 685 s, 623 s, 575  $\text{cm}^{-1}$ . Anal. Calcd for  $\text{C}_{30}\text{H}_{86}\text{N}_4\text{-SrSi}_8\text{Se}_2$ : C, 37.0; H, 8.91; N, 5.76. Found: C, 36.9; H, 9.29; N, 5.41.

**Sr[TeSi(SiMe<sub>3</sub>)<sub>3</sub>]<sub>2</sub>(THF)<sub>4</sub>.** Light yellow crystals were obtained from THF/hexanes (1:1) (25%). Mp: >300 °C.  $^1\text{H}$  NMR (400 MHz,  $\text{C}_6\text{D}_6$ ):  $\delta$  3.83 (m, 16 H), 1.54 (m, 16 H), 0.48 (s, 54 H).

**Sr[TeSi(SiMe<sub>3</sub>)<sub>3</sub>]<sub>2</sub>(pyridine)<sub>4</sub>.** Large yellow crystals were isolated from ether (75%). Mp: >300 °C.  $^1\text{H}$  NMR (300 MHz,  $\text{C}_6\text{D}_6$ ):  $\delta$  9.35 (d, 8 H), 6.80 (t, 4 H), 6.64 (t, 8 H), 0.48 (s, 54 H).  $^{125}\text{Te}\{^1\text{H}\}$  NMR ( $\text{C}_6\text{D}_6$ ):  $\delta$  -1482 (s). IR: 1594 m, 1573 w, 1488 w, 1445 s, 1238 s, 1150 m, 1066 m, 1033 m, 1001 m, 836 vs, 749 m, 701 s, 618  $\text{cm}^{-1}$ . Anal. Calcd for  $\text{C}_{38}\text{H}_{74}\text{N}_4\text{Si}_8\text{SrTe}_2$ : C, 39.5; H, 6.46; N, 4.85. Found: C, 39.4; H, 6.45; N, 4.75.

**Ba[SeSi(SiMe<sub>3</sub>)<sub>3</sub>]<sub>2</sub>(TMEDA)<sub>2</sub>.** An off-white crystalline solid was obtained from hexanes (69%). Mp: 285–286 °C.  $^1\text{H}$  NMR (300 MHz,  $\text{C}_6\text{D}_6$ ):  $\delta$  2.24 (s, 24 H), 2.14 (s, 8 H), 0.41 (s, 54 H). IR: 1377 s, 1294 s, 1180 w, 1160 m, 1131 m, 1099 w, 1075 m, 1034 s, 1019 m, 950 m, 925 w, 866 sh, 836 s, 780 m, 741 w, 685 s, 622 s, 575  $\text{cm}^{-1}$ .

**Ba[TeSi(SiMe<sub>3</sub>)<sub>3</sub>]<sub>2</sub>(THF)<sub>4</sub>.** Light yellow crystals were obtained from THF/hexanes (1:3) (52%). Mp: >300 °C.  $^1\text{H}$  NMR (400 MHz,  $\text{C}_6\text{D}_6$ ):  $\delta$  3.73 (m, 16 H), 1.48 (m, 16 H), 0.52 (s, 54 H).

**Ba[TeSi(SiMe<sub>3</sub>)<sub>3</sub>]<sub>2</sub>(pyridine)<sub>5</sub>.** Large yellow crystals were isolated from pyridine (73%). Mp: 162–165 °C.  $^1\text{H}$  NMR (400 MHz,  $\text{C}_6\text{D}_6$ ):  $\delta$  9.14 (d, 10 H), 6.82 (t, 5 H), 6.66 (t, 10 H), 0.52 (s, 54 H).  $^{125}\text{Te}\{^1\text{H}\}$  NMR ( $\text{C}_6\text{D}_6$ ):  $\delta$  -1405 (s). IR: 1615 w, 1588 m, 1574 m, 1446 s, 1235 s, 1146 m, 1066 m, 1029 m, 997 m, 832 vs, 745 s, 697 s, 684 s, 615  $\text{cm}^{-1}$ . Anal. Calcd for  $\text{C}_{43}\text{H}_{79}\text{N}_5\text{Si}_8\text{BaTe}_2$ : C, 40.2; H, 6.20; N, 5.46. Found: C, 39.9; H, 6.19; N, 5.10.

**X-ray Crystallography.** Our standard operating procedures were followed.<sup>14</sup> The structures were solved by the Patterson method and refined via least-squares and Fourier techniques. Crystals were grown from the solvents indicated, covered with Paratone-N oil and transferred to an Enraf-Nonius CAD-4 diffractometer. Table 2 contains the details of the crystallographic data collection parameters. Dr. F. J. Hollander, Staff Crystallographer of the U.C. Berkeley Crystallography facility (CHEXRAY), determined the structures of the tellurolate derivatives. Supplementary data for the structures of  $\text{Mg}[\text{TeSi}(\text{SiMe}_3)_3]_2(\text{THF})_2$  and  $\text{Ca}[\text{TeSi}(\text{SiMe}_3)_3]_2(\text{THF})_4$  were deposited earlier.<sup>9</sup>

**Mg[SeSi(SiMe<sub>3</sub>)<sub>3</sub>]<sub>2</sub>[TRMPSI].** Large transparent block-shaped crystals were grown from HMDSO. Automatic peak search and indexing procedures yielded a primitive monoclinic cell. Inspection of the systematic absences indicated the space group  $P2_1/n$ . During data collection, a large fluctuation in temperature caused a temporary loss of intensity. The reflections collected during this fluctuation (764) were rejected on the basis of the intensity standards following a nonlinear isotropic decay correction. Hydrogen atoms were assigned idealized locations and were included on structure factor calculations, but were not refined. The final residuals for 400 variables against 2110 data for which  $F^2 > 2.5\sigma(F^2)$  were  $R = 0.0784$ ,  $R_w = 0.0630$ , and  $\text{GOF} = 1.367$ .

**Sr[SeSi(SiMe<sub>3</sub>)<sub>3</sub>]<sub>2</sub>(TMEDA)<sub>2</sub>.** Small platelike crystals were grown from hexanes. Automatic peak search and indexing procedures yielded a primitive monoclinic cell. Inspection of the systematic absences indicated the space group  $P2_1/c$ . Hydrogen atoms were assigned idealized locations and were included on structure factor calculations, but were not refined. The final residuals for 205 variables against 1739 data for which  $F^2 > 3\sigma(F^2)$  were  $R = 0.0484$ ,  $R_w = 0.0439$ , and  $\text{GOF} = 1.27$ .

**Mg[TeSi(SiMe<sub>3</sub>)<sub>3</sub>]<sub>2</sub>(THF)<sub>2</sub>.** Large pale yellow plate-like crystals were grown from hexanes/THF. Automatic peak search and indexing procedures yielded a triclinic cell. Refinement in the space group  $P1$  yielded satisfactory results. Hydrogen atoms were assigned idealized locations and were included on structure factor calculations, but were not refined. In the final cycles of refinement, a secondary extinction parameter<sup>33</sup> was included (maximum correction = 8.5% on  $F$ ). The final residuals for 353 variables against 5519 data for which  $F^2 > 3\sigma(F^2)$  were  $R = 0.0254$ ,  $R_w = 0.0329$ , and  $\text{GOF} = 1.60$ .

**Ca[TeSi(SiMe<sub>3</sub>)<sub>3</sub>]<sub>2</sub>(THF)<sub>4</sub>.** Large clear yellow block-shaped crystals were grown from hexanes/THF. Automatic peak search and indexing procedures yielded a triclinic cell. Refinement in the space group  $P1$  yielded satisfactory results. Hydrogen atoms were assigned idealized locations and were included on structure factor calculations, but were not refined. Before final refinement, two reflections with abnormally large weight difference values were given zero weight. In the final refinement cycles, a secondary extinction parameter<sup>33</sup> was included (maximum correction = 6% on  $F$ ). The final residuals for 222 variables against 5377 data for which  $F^2 > 3\sigma(F^2)$  were  $R = 0.0332$ ,  $R_w = 0.0439$ , and  $\text{GOF} = 1.92$ .

**Ba[TeSi(SiMe<sub>3</sub>)<sub>3</sub>]<sub>2</sub>(pyridine)<sub>5</sub>.** Large yellow block-shaped crystals were grown from pyridine. Automatic peak search and indexing procedures yielded a monoclinic  $C$ -centered cell. Inspection of the systematic absences indicated the space group  $C2/c$ . Hydrogen atoms were assigned idealized locations and were included on structure factor calculations, but were not refined. The final residuals for 268 variables against 3674 data for which  $F^2 > 3\sigma(F^2)$  were  $R = 0.0293$ ,  $R_w = 0.0316$ , and  $\text{GOF} = 1.17$ .

**Acknowledgment.** We are grateful to the National Science Foundation (Grant No. CHE-9210406) for financial support, to Dow Chemical for the award of a graduate fellowship to D.E.G., and to the Alfred P. Sloan Foundation for the award of a research fellowship to J.A.

**Supplementary Material Available:** Tables of temperature factor expressions, positional parameters, intramolecular distances and angles, least-squares planes, and anisotropic thermal parameters for all structures (23 pages). Ordering information is given on any current masthead page.